JCTC Journal of Chemical Theory and Computation

Computational Study of Aqueous Reactions in Tocopherol Regeneration

R. Lui[†] and A. L. Cooksy*[,†,‡]

Department of Chemistry, San Diego State University, San Diego, California 92182-1030, and Centro de Graduados e Investigacion, Instituto Tecnológico de Tijuana, Apdo Postal 1166, Tijuana, B.C. México

Received July 3, 2006

Abstract: The α-tocopheroxyl radical, resulting from the scavenging of the peroxyl radical by α-tocopherol (vitamin E) in the cell membrane, will further react with the peroxyl radical to form tocopherones. A computational study is presented of the aqueous proton-transfer reactions of the α-8a-(hydro-dioxy)tocopherone and α-8a-(methyl-dioxy)tocopherone to produce 1-benzopyrylium, the subsequent hydrolysis to 2H-1-benzopyran-6(8aH)-one, and the terminating rearrangement of 8a-hydroxytocopherone to 2,5-cyclohexadiene-1,4-dione. The alkyl tail of true tocopherol is replaced by methyl in these studies. Calculations of the structures and energies along the reaction pathways were first performed at the BP86/TZVP/DGA1 level with a COSMO solvent model, and additional solvent corrections from COSMO-RS theory were subsequently added. The proposed mechanism is found to be thermodynamically and kinetically feasible in water. The ion-mediated steps are found to have free-energies of activation under 3 kcal mol^{-1}, with kinetics likely to be diffusion-limited. The unimolecular rearrangement is the slow step, with a predicted reaction rate constant of 0.056 min^{-1} at 298 K, in excellent agreement with the experimental value of 0.046 min^{-1}. Kinetic and thermodynamic properties of the ion-mediated steps are shown to rely strongly on the use of an accurate continuum solvation model. Distinct entropy and enthalpy contributions are determined from the temperature dependence of the predicted free energies.

1. Introduction

Vitamin E is a fat-soluble vitamin, existing in nature as any of eight different tocols and tocotrienols. All of these structures consist of a chromanol heterocycle (Figure 1) with a hydrophilic hydroxyl group at the 6 position and a hydrophobic alkyl tail at the 2 position, the latter anchoring the vitamin in cell membranes. This dual solubility enhances its antioxidant activity by protecting the lipid bilayers of cell membranes against reaction with free radicals.[1] In the vitamin E family, α-tocopherol (α-TH), a trimethyl-substituted tocol, is found to be the most biologically significant form and has been widely used to study the activity of vitamin E.

To consume destructive lipid peroxyl (LOO•) radicals, α-TH transfers the hydroxyl hydrogen to generate LOOH either by direct hydrogen transfer or sequential electron−proton transfers. The resulting tocopherol radical (T•) is less reactive than LOO• or the lipid radical (L•), because the conjugated π system in the chromanol ring system confers the T• with extra stability. In general, it is believed that T• will regenerate back to TH by reaction in the cell with vitamin C. Research[2] has indicated the enhancement of TH regeneration in the presence of other cooperative antioxidants, in particular, with the water-soluble vitamin C.[3,4] However, some of the T• generated in antioxidation will not regenerate but will further react with another ROO• to form 8a-(alkyldioxy)tocopherones.

Several computational studies of the antioxidant activity of tocopherol were carried out in the early 1990s,[5−9] and that field is now being extensively revisited.[10−16] To our

* Corresponding author fax: (619) 594-4634; e-mail: acooksy@sciences.sdsu.edu.

[†] San Diego State University.

[‡] Instituto Tecnológico de Tijuana.

10.1021/ct600161w CCC: $33.50
Published on Web 08/19/2006

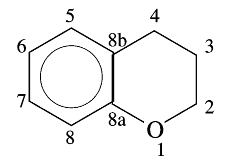

Figure 1. Position labels on the chromanol system.

knowledge, there has been no prior investigation by computational means of the subsequent reactions of tocopherol, including those that may lead to regeneration of the vitamin. One mechanism for the chemical recycling of tocopherol was proposed and studied by Liebler and co-workers,[17−19] with the steps illustrated in Scheme 1 for a model chromanol system. They proposed that the acid-catalyzed loss of the 8a-(alkyldioxy) in reaction 1 will lead to 1-benzopyrylium (α-T^+)[17] and that this can then be reduced by ascorbic acid directly back to α-TH. However, α-T^+ may also reversibly hydrolyze in reaction 2 to 8a-hydroxytocopherone (α-TOH), which then rearranges in reaction 3 to 2,5-cyclohexadiene-1,4-dione (α-TQ). The formation mechanism and relative stability in solution of the α-T^+ cation has recently been investigated in detailed experiments by Webster and co-workers.[20]

This work is a computational investigation of that mechanism. The specific reactions modeled are shown as reactions 1a, 1b, 2, and 3 in Scheme 1. The goal of this work has been to develop a computational model of these reactions to assess the feasibility of this proposed mechanism in an aqueous medium. Although this is not expected to be a major pathway in the cell membrane, these reactions may be significant in laboratory studies of vitamin E, particularly those that take place in the absence of the vitamin C or hydroquinone needed to regenerate the TH.

2. Methods

The chromanol ring of vitamin E consists of 12−15 heavy atoms (carbon or oxygen), depending on the number of methyl substituents. The tocopherol or tocotrienol then needs 16 additional heavy atoms to form the long alkyl tail. To reduce the conformational complexity of the system, these calculations focus on the chemically relevant chromanol ring system, replacing the long alkyl tail with a single methyl group. The resulting initial structure α-TH consists of only 16 heavy atoms, and there are then no more than six single-bond torsional modes connected to the chromanol system at any point in the reaction until the final ring-opening step in reaction 3.

Reaction 1 begins with our model 8a-(alkyl-dioxy)-tocopherone (α-TOOR), which is one possible product from the tocopherol antioxidizing reaction. It is simulated to interact with a hydronium ion (H_3O^+) in water, resulting in a α-T^+ and a corresponding alkyl-peroxide (HOOR). In Liebler et al.'s studies,[18] 8a-[(2,4-dimethyl-1-nitrilopent-2-yl)dioxy]tocopherone was used to study the hydrolysis and reduction of α-TOOR in acetonitrile/buffer mixtures. In the present work, the R substituents in the alkyl peroxide are chosen to be hydrogen (reaction 1a) and methyl (reaction 1b).

Scheme 1

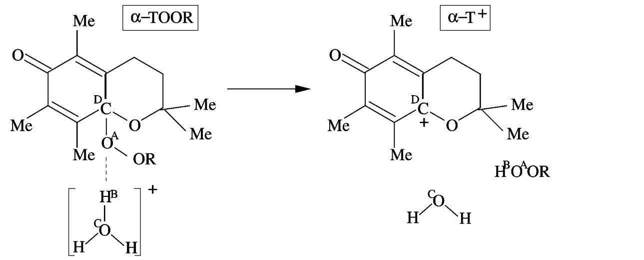

Reaction 1(a, b): R=H for Reaction **1a**, R=Me for Reaction **1b**.

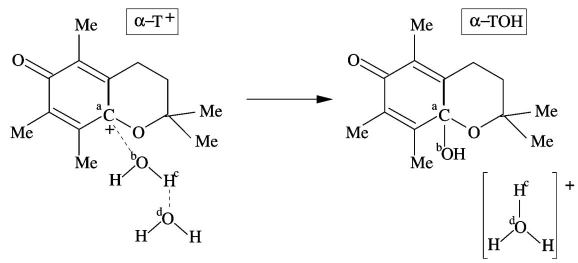

Reaction **2**.

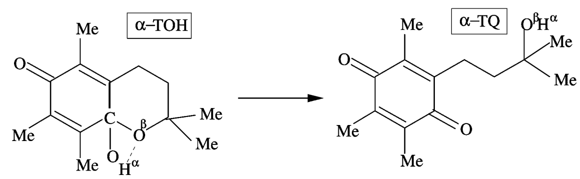

Reaction **3**.

For reaction 2, α-T^+ reacts with two water molecules, generating an α-TOH and an H_3O^+. In general, α-TOOR, α-T^+, and α-TOH can be reduced by vitamin C back to α-TH, but the present study has been restricted to smaller and more computationally tractable reaction systems. For reaction 3, the α-TOH generated from reaction 2 will rearrange to α-TQ, by opening the chromanol ring as shown. Reaction 3 is the terminal reaction studied in this project, because the resulting α-TQ is not regenerated back to α-TH. Studies of the antioxidant activity of α-TQ indicate that α-TQ is reduced to α-tocopherylhydroquinone (α-TQH_2) by enzymes or other hydroquinones. The α-TQH_2, which can scavenge free radicals by hydrogen transfer, may then function as an antioxidant in lipids.[21−24]

Initial probes of the chemistry were carried out at the BP86 density functional level of theory,[25,26] using the COSMO solvent model[27] to incorporate the fundamental electrostatic interactions with water. The Dunning−Huzinaga TZVP basis set was used with DGA1 as the density fitting approximation.[28,29] The geometry optimization is the most time-consuming process, and the calculation has to be done for each point on the reaction surface.

The strong interactions inherent in aqueous ionic chemistry require a more accurate solvent model, and the results of the BP86/COSMO calculations were then corrected by the COSMO-RS method of Klamt et al.[30−32] This correction accounts for structural and thermal variations in the intermolecular forces and predicts relative aqueous ion free energies within roughly 1 kcal mol^{-1} of the experimental values. The COSMO-RS corrections were applied at 298 and 310 K.

Table 1. Summary of Parameters in Partial Optimizations

reaction	reaction coordinate	min	max	number of points
1a	r_{AB}	1.1 Å	1.9 Å	41
1b	r_{AB}	1.1 Å	1.8 Å	45
2	r_{ab}	1.4 Å	2.7 Å	47
3	$r_{\alpha\beta}$	1.0 Å	2.4 Å	18

In this process, the transition state of the reaction cannot be located by analytical methods, because the COSMO-RS correction is applied in a computational step distinct from the geometry optimization. Hence, for each reaction, one bond length was selected as the effective reaction coordinate (r), and the free energy was calculated at discrete points along this coordinate. At each of these points, corresponding to some fixed value of the reaction coordinate, the remaining geometric parameters were optimized to minimize the vibrational potential energy. At least 40 points along this coordinate were calculated for each of reactions 1a, 1b, and 2. Reaction 3, as explained below, is less sensitive to the solvent model and was comparably modeled with only 18 points. The parameters for these series are summarized in Table 1. The r values generally range from a minimum near the corresponding chemical bond length and a maximum near 2 Å. The maximum r value is limited by the COSMO solvent model's description of the molecular system using a single solvent cavity, an increasingly inappropriate representation as r exceeds the effective diameter of the solvent molecule.

For reactions 1a and 1b, the bond length between O^A and H^B (r_{AB}) was initially chosen as the effective reaction coordinate, anticipating that both of the other bonds heavily featured in the reaction, O^CH^B and O^AC^D, would be strongly coupled to r_{AB}. The reaction coordinate for 2 was r_{ab}, the separation between the bridging carbon 8a on the chromanol ring and the oxygen from a neighboring water molecule. In the unimolecular reaction 3, the reaction coordinate was the distance $r_{\alpha\beta}$ between the chromanol oxygen atom and a hydrogen atom transferred as the ring opens. In each case, the reaction coordinate decreases, approaching a chemical bond length, as the reaction progresses.

The free energies reported in this work are based on a combination of the electronic energy calculations and the COSMO-RS solvent free energy correction. This sum neglects the entropic contribution to the free energy from the internal vibrations of the molecule, and in some cases, this contribution is critical. The reaction free energies ΔG_v° include approximate vibrational contributions, obtained by carrying out a distinct harmonic frequency analysis on the isolated reactants and products of each reaction. We have not attempted to carry out the vibrational analysis on the transition states because, for reactions 1 and 2, the transition states are stationary points on the reaction diagram only after the COSMO-RS correction is applied. The typical harmonic analysis is invalid at nonstationary point geometries, and a numerical frequency calculation including the COSMO-RS correction is prohibitive.

The Gaussian 03 program suite[33] was used for all geometry optimizations, including the COSMO solvent model, and for the vibrational calculations. These calculations were carried out on a variety of Intel Pentium-based computers running Linux. With processor speeds of roughly 1−2.5 GHz, the geometry optimizations typically required 4−5 days of real time on a single dedicated computer node. Despite the simplified structure of our model tocopherol, convergence of the calculations at geometries near the transition state was often slowed by the difficulty in optimizing relative positions of weakly interacting chemical components. In particular, the potential energy is fairly insensitive to the orientation of the H_3O^+ in reaction 1. Minimum memory requirements were roughly 25 MW. The COSMO-RS calculations were carried out with the program COSMOtherm running on an Intel-processor PC.[34]

Table 2. Computed Free Energies and Enthalpies (kcal mol^{-1}), Entropies (cal K^{-1} mol^{-1}), and Equilibrium Constants

reaction	1a	1b	2	3
ΔG° (298 K)	−3.29	−1.73	−0.40	−5.67
ΔG_v° (298 K)	−4.72	−1.60	3.80	−11.13
K (298 K)	$2.90\cdot10^3$	14.9	1.63×10^{-3}	$6.37\cdot10^7$
$\Delta G^\ddagger$ (298 K)		1.82	2.80	21.50
ΔG° (310 K)	−4.12	−2.58	0.42	−5.67
ΔG_v° (310 K)	−5.44	−2.21	4.60	−11.13
K (310 K)	$6.84\cdot10^3$	36.1	5.71×10^{-4}	$3.18\cdot10^7$
$\Delta G^\ddagger$ (310 K)		1.44	2.90	21.50
ΔH°	17.9	18.2	−16.6	−5.67
ΔS°	69.2	66.5	−68.3	0.00

3. Results

The standard Gibbs free energies (G°) calculated from COSMOtherm at both 298 and 310 K were plotted against the selected reaction coordinate. From these curves, the free energies of activation were estimated. Overall ΔG°, ΔH°, and ΔS° values were calculated instead from the COSMO-RS-corrected free energies of the isolated reactants and products, with equilibrium constants approximated by the equilibrium relation

$$K = \exp[-\Delta G^\circ/(RT)] \quad (1)$$

and enthalpies and entropies of reaction estimated from the differences between results at 298 and 310 K. These results are summarized for all of the reactions in Table 2. The following sections discuss characteristics specific to the individual reactions.

Reaction 1. In reaction 1a, α-TOOH reacts with a H_3O^+ molecule to form α-T^+, hydroperoxide (H_2O_2), and a water molecule, while for reaction 1b, α-TOOMe reacts with a H_3O^+ to form α-T^+ and methylperoxide (HOOMe) with H_2O. In the lowest energy structures, both α-TOOH and α-TOOMe are bicyclic with the OOH/OOMe group perpendicular to the chromanol ring. For α-TOOH, the two oxygen atoms have partial negative charges, and the OOC group in the methylperoxyl are partially negative for α-TOOMe. In both reactants, the π-conjugated ring is slightly positive and the charge is broadly distributed around the ring. Within the peroxyl group, O^A has the most negative formal charge and is the likeliest site of attack by the hydronium to initiate the reaction.

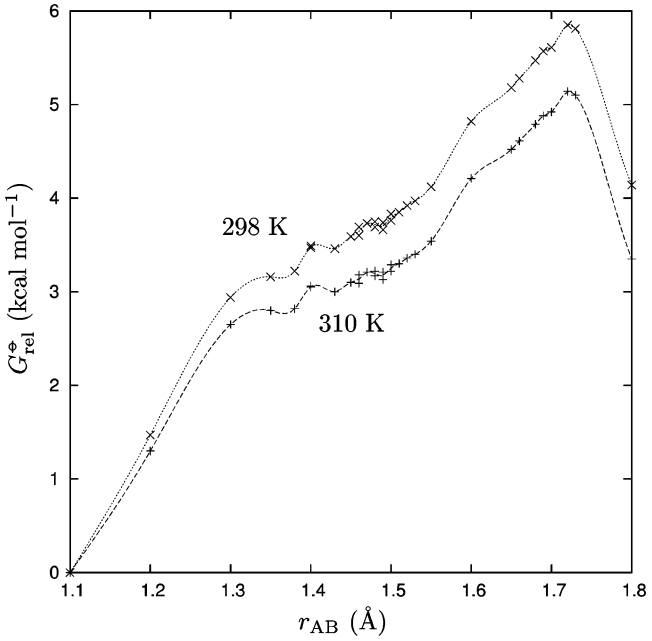

Figure 2. Reaction 1a: Relative standard Gibbs free energy versus r_{AB}.

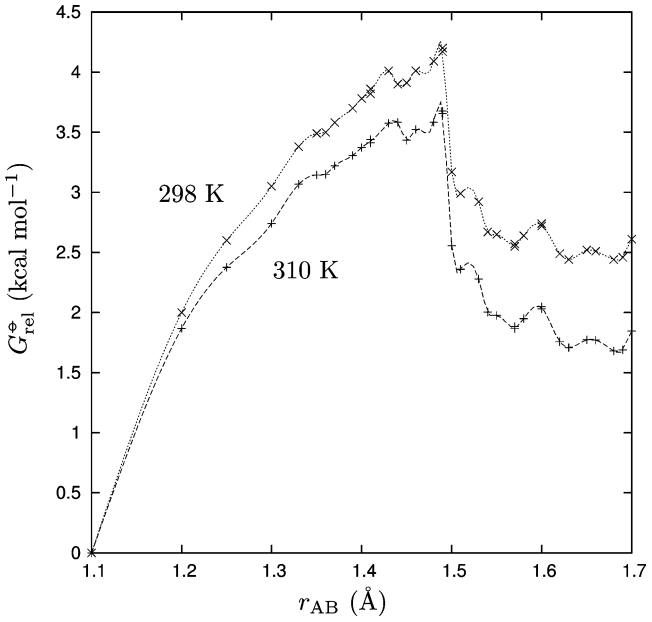

Figure 3. Reaction 1b: Relative standard Gibbs free energy as a function of O^AH^B separation.

The relative free energies are plotted in Figures 2 and 3. In these and subsequent free energy graphs, the combined energy of the reactants at maximum separation is chosen as the reference point. Note that the direction of the reaction in these graphs proceeds from right (large r) to left. The small variations in the curves are consistent with expected variations in the extent to which the convergence criteria are satisfied. In reaction 1a, the uncorrected COSMO calculations predict a fairly flat energy profile as r_{AB} initially decreases in these calculations. With the addition of the COSMO-RS correction, a shallow local minimum appears at $r_{AB} = 1.76$ Å. Here, the system has a free energy of -0.41 or -0.48 kcal/mol (at 298 and 310 K, respectively). The curve then suddenly jumps in free energy by roughly 2.5 kcal/mol. The discontinuity in Figure 2 occurs between r_{AB} values of 1.74 and 1.76 Å and is a common consequence of parametrizing the reaction coordinate using a single bond length. At this same point, the C−O bond length r_{AD} increases suddenly by 0.4 Å, indicating that, near the transition state, the true reaction coordinate depends heavily on this bond length. A survey of the free energy at 12 points as a function of r_{AB} and r_{AD} near this geometry confirms that the transition state for the reaction is at the geometry corresponding to $r_{AB} = 1.74$ Å in Figure 2. Similar difficulties involving the selection of the reaction coordinate do not appear in the other reactions studied.

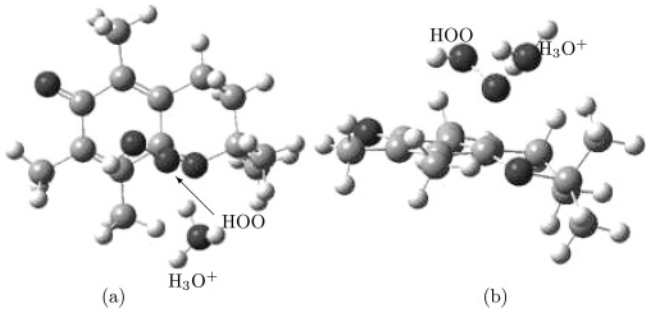

Figure 4. Approximate reaction 1a transition state geometry, viewed (a) from above the chromanol plane and (b) with the chromanol edge-on.

The transition state of reaction 1b is identifiable at $r_{AB} = 1.435$ Å, with a relative free energy of 1.83 kcal/mol at 298 K and 1.44 kcal/mol at 310 K. Both reactions are mildly spontaneous, with negative ΔG° values of magnitudes less than 5 kcal/mol.

For both reactions 1a and 1b, Table 2 shows that $\Delta G^{\circ} < 0$ at both temperatures, with the equilibria lying strongly on the product side. However, a comparison of Figures 2 and 3 shows that reaction 1a has a greater drop in free energy than reaction 1b. This may be due to the hydrogen bond being more likely to form between H_2O_2 and water than between CH_3OOH and water. Both reactions have similar products, differing only in the nature of the peroxide. Because the methyl group is more electronegative than the hydrogen, the methyl group donates electrons to the oxygen less effectively, and this causes the oxygen to be less negatively charged. The charge on O^A is -0.31 e at $r_{AB} = 1.1$ Å in reaction 1a, slightly higher than the corresponding value of -0.28 for reaction 1b, while the charges at H^B are the same in both reactions. This results in a reduced hydrogen bond strength for the methylperoxide and, therefore, less stabilization in an aqueous solvent. Hydrogen bonds usually contribute to stronger intermolecular forces, or a lower G° in this case.

The electron-donating effect from the methyl group is also reflected in the bond strength of the O^AC^D bond, which requires a smaller r_{AB} value before breaking. In the transition state, bonds are breaking between O^A and C^D and between H^B and O^C, while a new bond is being formed between O^A and H^B. The transition state geometry for reaction 1a is shown in Figure 4 and lies at approximately $r_{AB} = 1.74$ Å. For reaction 1b, the transition state is at $r_{AB} = 1.47$ Å.

Reaction 1b thermodynamically favors the product side. This is driven by the formation of α-T^+, which stabilizes

the charge in the π-conjugated system, and the increase in entropy by the increase of the number of moles in the product. The effects of the temperature difference are small, with $G°$ values shifting by less than 1 kcal/mol between reactions at both temperatures. Without the COSMO-RS correction, a curve with no barrier is obtained. The COSMO-RS correction has its greatest effect in these calculations by stabilizing the H_3O^+ moiety. In contrast to the other principal cation, α-T^+, for which the ring's π-conjugated system contributes charge delocalization, the charge on H_3O^+ is strongly localized and gains most from a more adaptable solvent model.

Applying the conditions pH = 3.6 and 298 K from Liebler et al.'s study,[18] the rate constant can in principle be calculated from the free energy of activation, $\Delta G^‡$, using the Eyring equation from elementary transition state theory. The Eyring equation for a bimolecular reaction has a general form

$$k = \frac{k_B T}{hC} \exp[-\Delta G^‡/(RT)]$$

where C is 55.6 mol L^{-1} for aqueous reactions. To put this in the form of the first-order rate constant quoted by Liebler et al., this value is multiplied by the H_3O^+ concentration. The first-order rate constant of reaction 1b at 298 K, k'_{1b}, is then calculated to be 8.0×10^7 min^{-1}. This value greatly exceeds the diffusion-limited collision rate, on the of order 1 min^{-1}, indicating that Liebler et al.'s value of 0.296 min^{-1} arises fully from diffusion-limited kinetics.

Reaction 2. In reaction 2, α-T^+ reacts with two water molecules to form α-TOH and an H_3O^+. In the optimized α-TOH structure, the attached OH group is perpendicular to the π-conjugated ring, while the other side of the chromanol ring is bent. As was the case for reaction 1b, the COSMO-RS correction is again critical to locating a transition state. In the absence of this correction, the free energy climbs without barrier from reactants to products, as shown for the COSMO curve in Figure 5, and indeed the product instability would then be predicted to halt the reaction at this step. Once the correction is added, the relative free energy of the products drops by 9 kcal mol^{-1}, again driven by the differential stabilization of H_3O^+ relative to α-T^+. The transition state appears at $r_{ab} \approx 1.9$ Å, as the oxygen atom of one water molecule moves toward the C^a of the ring while a hydrogen rotates to hydrogen-bond to an adjacent water molecule (H^c–O^d in Scheme 1), with the geometry shown in Figure 6. The O^bH^c bond lengthens significantly at $r_{ab} = 1.6$ Å, indicating that the proton shift of H^c from O^b to O^d occurs before the transition state is reached. The optimized value r_{ab} of α-TOH is 1.45 Å, leading to a local minimum in Figure 5 as this distance approaches 1.40 Å.

One could expect the charge in α-T^+ to be delocalized along the π-conjugated system of the chromanol ring. However, the charges around the chromanol of α-T^+ predicted by the electronic structure calculations, listed in Table 3, predict the positive charge to be concentrated at position 8a in Figure 1. Therefore, it is reasonable to assume that the electronegative O^b approaches this site to initialize the reaction. As shown in Figure 7, the charge on the ring system drops smoothly throughout the reaction, as the charge transfers briefly to the OH group (peaking at $r_{ab} = 1.6$ Å) before its redistribution ultimately to the hydronium group.

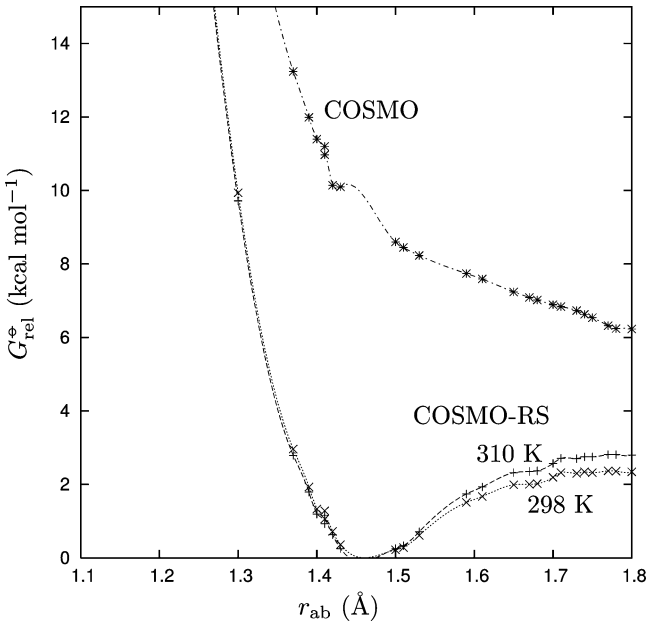

Figure 5. Reaction 2: Relative standard Gibbs free energy as a function of C^aO^b separation.

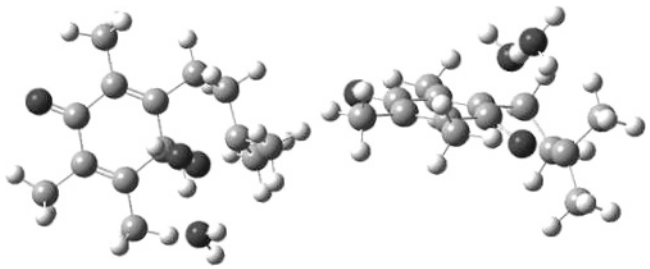

Figure 6. Approximate reaction 2 transition state geometry, viewed from two angles.

Table 3. Relative Charges around the Chromanol Ring in α-T^+

atom	relative charge	atom	relative charge
O1	−0.07	C2	−0.02
C3	0.12	C4	0.13
C5	−0.03	C6	0.21
C7	0.06	C8	−0.14
C8a	0.36	C8b	0.08

Unlike reaction 1, the results in Table 2 show that reaction 2 has $\Delta G° > 0$ at both temperatures, and the predicted equilibrium for this hydration reaction lies strongly on the reactant side. The entropy decrease, driven by the loss of free water, overwhelms the exothermicity which results from the C–O bond formation. However, for both reactions 1 and 2, the free energy of activation $\Delta G^‡$ is less than 3 kcal mol^{-1}, indicating that the kinetics of these reactions will be determined instead by the diffusion-limited collision rates in solution, in agreement with Liebler et al.'s qualitative observations.

Reaction 3. The relative free energies for reaction 3 are plotted in Figure 8 as a function of the $H^\alpha O^\beta$ separation. In

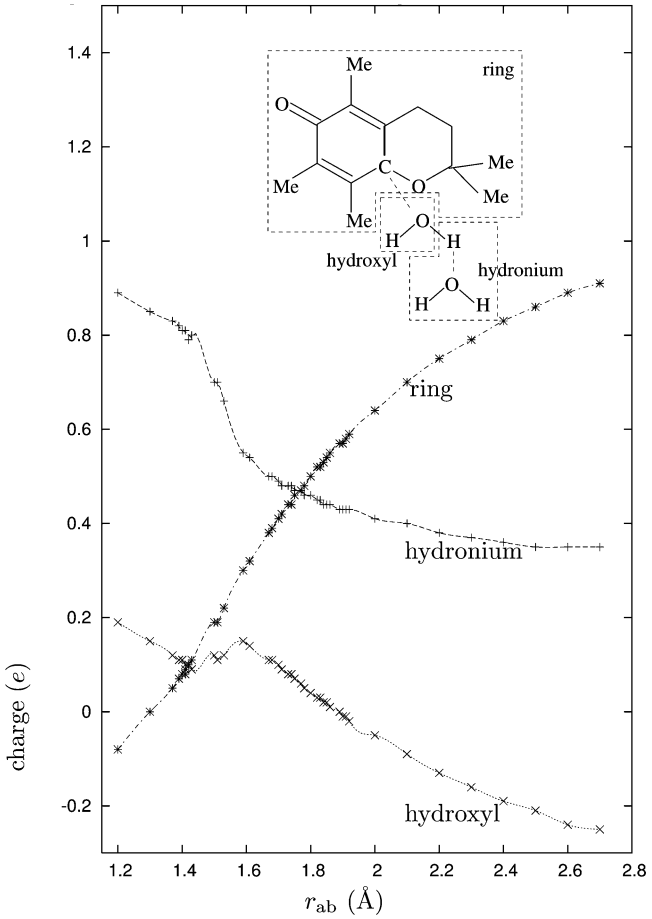

Figure 7. Reaction 2: Charges on various species.

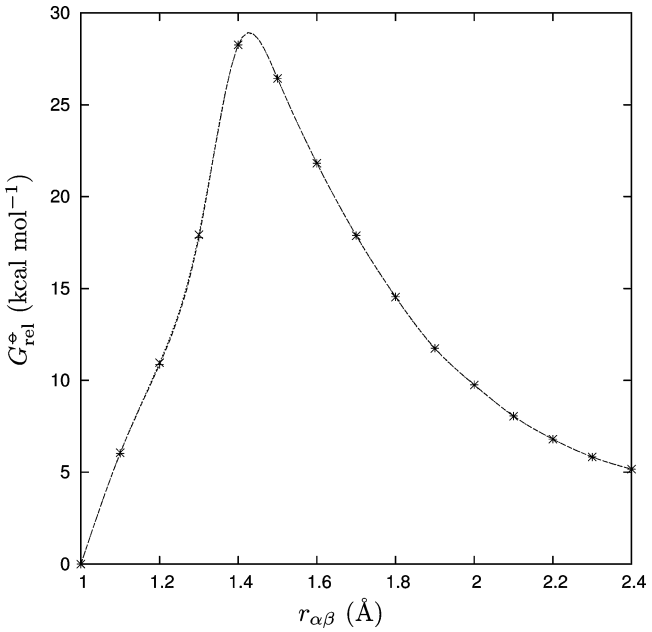

Figure 8. Reaction 3: Relative standard Gibbs free energy as a function of $H^{\alpha}O^{\beta}$ separation. Results at both 298 and 310 K are graphed but not visibly distinguishable at this scale.

reaction 3, α-TOH rearranges to α-TQ by opening the ring. During the rearrangement, bonds are broken between O^{δ} and H^{α} and between C^{γ} and O^{β}. At the same time, a bond forms between O^{β} and H^{α} and a double bond between C^{γ} and O^{δ}. The transition state structure, with H^{α} pointing toward the chromanol O^{δ}, is shown in Figure 9. At this geometry, where $r_{\alpha\beta} \approx 1.4$ Å, the optimized values of $r_{\gamma\beta}$ and $r_{\alpha\delta}$ increase sharply, indicating that those bonds are breaking. The long tail attached to the quinone is then free to move and rotate away from the remaining monocycle. At the same time, the $r_{\gamma\delta}$ drops from approximately 1.44 Å to 1.25 Å, which corresponds to the change from a single bond to a double bond.

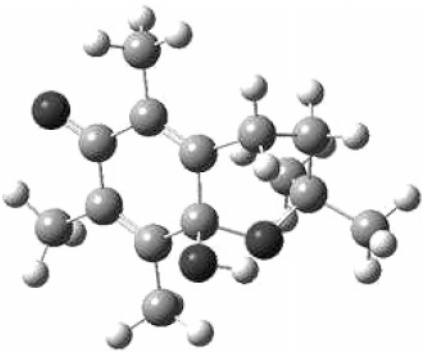

Figure 9. Approximate reaction 3 transition state geometry.

Table 2 indicates that the reaction equilibrium lies strongly on the product side. Unlike the previous reactions, the COSMO-RS correction exerts very little effect on the free energies for reaction 3 at either temperature; the differences with and without the correction average to only 0.20 kcal/mol across the sampled points. The vibrational correction to the free energy is also much greater for reaction 3 than for the other two reactions, as expected from the substantial increase in vibrational entropy associated with the ring opening.

Employing the Eyring equation for a unimolecular reaction, the rate constant of reaction 3, k_3, is determined to be 0.056 min^{-1}. A comparison with the value of 0.046 min^{-1} from Liebler et al. for the corresponding reaction shows that the results are compatible. This encouraging agreement is likely to be in some part fortuitous, because no vibrational correction has been applied to the transition state. However, the Eyring equation should be more successful here than in the higher-order reaction 1 and reaction 2, because fewer assumptions are necessary in the unimolecular case. In addition, the insensitivity of the free energy curve to solvent corrections indicates that the neglect of solvent interactions (such as diffusion and cage effects) in the Eyring equation should be less of a problem for reaction 3.

4. Conclusion

Neglecting vibrational corrections, the formation of α-TQ from α-TOOH is predicted to have an overall equilibrium constant of 3.01×10^8 at 298 K and 1.24×10^8 at 310 K. When the reactant in step 1 is replaced with α-$TOOCH_3$, the overall equilibrium constants are estimated to be 1.54×10^6 and 6.55×10^5 for temperatures 298 and 310 K, respectively. These results indicate that the overall reaction of α-TOOR to α-TQ is thermodynamically favorable, lying strongly on the product side in the absence of additional reactants such as vitamin C.

Liebler et al. measure the formation of α-TQ from α-TOOR as having an effective first-order reaction rate constant $k_{overall} = 0.036\ min^{-1}$.[18] The formation of α-TQ takes place via three sequential reactions:

$$\alpha\text{-TOOR} + H_3O^+ \xrightarrow{k_1} \alpha\text{-T}^+ + \text{ROOH} \quad (2)$$

in which the effective first-order rate constant k_1' was

$$\alpha\text{-T}^+ + 2H_2O \xrightarrow{k_2} \alpha\text{-TOH} + H_3O^+ \quad (3)$$

$$\alpha\text{-TOH} \xrightarrow{k_3} \alpha\text{-TQ} \quad (4)$$

estimated to be 0.296 min^{-1}. The rate of hydrolysis of α-T^+ to α-TOH was too fast to determine, whereas the rate of arrangement of α-TOH to α-TQ, k_3, was found to be 0.046 min^{-1}.

Because both reactions 1 and 2 have small free energy barriers of around 4 kcal/mol, they are both kinetically facile at these temperatures. Of these, the effective rate constant k_2' is predicted to be greater than k_1' because, in the pseudo-first-order limit, k_2' is proportional to the H_2O concentration and k_1' to the much lower H_3O^+ concentration:

$$k_2' \approx [H_2O]k_2;\ k_1' \approx [H_3O^+]k_1$$

This result, coupled with the relatively high activation energy barrier for reaction 3, predicts the ordering of the rate constants to be $k_3 < k_1' < k_2'$. This ordering is consistent with the results from Liebler et al.'s work, in which the rearrangement of α-TOH to α-TQ (reaction 3) is the rate-determining step of the overall reaction, and reaction 2 is the fast step.

The COSMO-RS solvent correction has proven to be a significant factor in predicting properties of this reaction pathway. The relative instability of H_3O^+ prior to the COSMO-RS correction would otherwise appear to halt the reaction at step 2. At present, this is only a qualitative result, because the activation barriers in the ion-mediated steps are not determined experimentally. Future work will attempt to assess the quantitative success of these methods in modeling ion-mediated biochemical systems.

Acknowledgment. The authors thank Dr. Andreas Klamt for kindly suppling the COSMOtherm license during the course of this project and for comments on the manuscript, William Root for extensive use of his computing facilities, and Prof. Pete Kovacic for valuable guidance. The authors are grateful to Dong Xu and Olga Noris for technical support. Funding was provided by the Blasker Fund of the San Diego Foundation and Grant CHE-0216563 of the National Science Foundation.

Supporting Information Available: Numerical free energy values and the geometries of the reaction endpoint and transition state species. This material is available free of charge via the Internet at http://pubs.acs.org.

References

(1) Traber, M. G.; Kayden, H. J. *Am. J. Clin. Nutr.* **1987**, *46*, 488−495.

(2) Buettner, G. R. *Arch. Biochem. Biophys.* **1993**, *300*, 535−543.

(3) Bisby, R. H.; Ahmed, S. *Free Radical Biol. Med.* **1989**, *6*, 231−239.

(4) Wang, X.; Quinn, P. J. *Mol. Membr. Biol.* **2000**, *17*, 143−156.

(5) Babbs, C. F.; Steiner, M. G. *Free Radical Biol. Med.* **1990**, *8*, 471−485.

(6) Nagaoka, S.; Okauchi, Y.; Urano, S.; Nagashima, U.; Mukai, K. *J. Am. Chem. Soc.* **1990**, *112*, 8921−8924.

(7) Nagaoka, S.; Kuranaka, A.; Tsuboi, H.; Nagashima, U.; Mukai, K. *J. Phys. Chem.* **1992**, *96*, 2754−2761.

(8) Nagaoka, S.; Sawada, K.; Fukumoto, Y.; Nagashima, U.; Katsumata, S.; Mukai, K. *J. Phys. Chem.* **1992**, *96*, 6663−6668.

(9) Nagaoka, S.; Mukai, K.; Itoh, T.; Katsumata, S. *J. Phys. Chem.* **1992**, *96*, 8184−8187.

(10) Wright, J. S.; Johnson, E. R.; DiLabio, G. A. *J. Am. Chem. Soc.* **2001**, *123*, 1173−1183.

(11) Leopoldini, M.; Marino, T.; Russo, N.; Toscano, M. *J. Phys. Chem. A* **2004**, *108*, 4916−4922.

(12) Rhodes, C. J.; Tran, T. T.; Denton, P.; Morris, H. *Free Radical Res.* **2002**, *36*, 89−90.

(13) Lucarini, M.; Mugnaini, V.; Pedulli, G. F.; Guerra, M. *J. Am. Chem. Soc.* **2003**, *125*, 8318−8329.

(14) Setiadi, D. H.; Chass, G. A.; Koo, J. C. P.; Penke, B.; Csizmadia, I. G. *THEOCHEM* **2003**, *666−667*, 439−443.

(15) Espinosa-Garcia, J. *Chem. Phys. Lett.* **2004**, *388*, 274−278.

(16) Rhodes, C. J.; Tran, T. T.; Morris, H. *Spectrochim. Acta, Part A* **2004**, *60*, 1401−1410.

(17) Liebler, D. C.; Burr, J. A. *Biochemistry* **1992**, *31*, 8278−8284.

(18) Liebler, D. C.; Kaysen, K. L.; Kennedy, T. A. *Biochemistry* **1989**, *28*, 9772−9977.

(19) Liebler, D. C.; Baker, P. F.; Kaysen, K. L. *J. Am. Chem. Soc.* **1990**, *112*, 6995−7000.

(20) Lee, S. B.; Lin, C. Y.; Gill, P. M. W.; Webster, R. D. *J. Org. Chem.* **2005**, *70*, 10466−10473.

(21) Liebler, D. C.; Burr, J. A. *Lipids* **2000**, *35*, 1045−1047.

(22) Kohar, I.; Baca, M.; Suana, C.; Stocker, R.; Southwell-Keely, P. T. *Free Radical Biol. Med.* **1995**, *19*, 197−207.

(23) Siegel, D.; Bolton, E. M.; Burr, J. A.; Liebler, D. C.; Ross, D. *Mol. Pharmacol.* **1997**, *52*, 300−305.

(24) Shi, H.; Nogichi, N.; Niki, E. *Free Radical Biol. Med.* **1999**, *27*, 334−346.

(25) Becke, A. D. *Phys. Rev. A: At., Mol., Opt. Phys.* **1988**, *38*, 3098−3100.

(26) Perdew, J. P. *Phys. Rev. B: Condens. Matter Mater. Phys.* **1986**, *33*, 8822−8824.

(27) Klamt, A.; Schürmann, G. *J. Chem. Soc., Perkin Trans. 2* **1993**, 799−805.

(28) Dunning, T. H. *J. Chem. Phys.* **1971**, *55*, 716−723.

(29) Godbout, N.; Salahub, D. R.; Andzelm, J.; Wimmer, E. *Can. J. Chem.* **1992**, *70*, 560−571.

(30) Klamt, A.; Jonas, V.; Bürger, T.; Lohrenz, J. C. W. *J. Phys. Chem. A* **1998**, *102*, 5074−5085.

(31) Klamt, A. *J. Phys. Chem.* **1995**, *99*, 2224−2235.

(32) Klamt, A.; Eckert, F.; Diedenhofen, M.; Beck, M. E. *J. Phys. Chem. A.* **2003**, *107*, 9380−9386.

(33) Frisch, M. J.; Trucks, G. W.; Schlegel, H. B.; Scuseria, G. E.; Robb, M. A.; Cheeseman, J. R.; Montgomery, J. A., Jr.; Vreven, T.; Kudin, K. N.; Burant, J. C.; Millam, J. M.; Iyengar, S. S.; Tomasi, J.; Barone, V.; Mennucci, B.; Cossi, M.; Scalmani, G.; Rega, N.; Petersson, G. A.; Nakatsuji, H.; Hada, M.; Ehara, M.; Toyota, K.; Fukuda, R.; Hasegawa, J.; Ishida, M.; Nakajima, T.; Honda, Y.; Kitao, O.; Nakai, H.; Klene, M.; Li, X.; Knox, J. E.; Hratchian, H. P.; Cross, J. B.; Adamo, C.; Jaramillo, J.; Gomperts, R.; Stratmann, R. E.; Yazyev, O.; Austin, A. J.; Cammi, R.; Pomelli, C.; Ochterski, J. W.; Ayala, P. Y.; Morokuma, K.; Voth, G. A.; Salvador, P.; Dannenberg, J. J.; Zakrzewski, V. G.; Dapprich, S.; Daniels, A. D.; Strain, M. C.; Farkas, O.; Malick, D. K.; Rabuck, A. D.; Raghavachari, K.; Foresman, J. B.; Ortiz, J. V.; Cui, Q.; Baboul, A. G.; Clifford, S.; Cioslowski, J.; Stefanov, B. B.; Liu, G.; Liashenko, A.; Piskorz, P.; Komaromi, I.; Martin, R. L.; Fox, D. J.; Keith, T.; Al-Laham, M. A.; Peng, C. Y.; Nanayakkara, A.; Challacombe, M.; Gill, P. M. W.; Johnson, B.; Chen, W.; Wong, M. W.; Gonzalez, C.; Pople, J. A. *Gaussian 03*, revision C.01; Gaussian, Inc.: Wallingford, CT, 2004.

(34) Klamt, A.; Eckert, F. *COSMOtherm*, version 2.1; COSMOlogic GmbH & Co., KG: Leverkusen, Germany, 2005.

CT600161W